MATERIALS CHEMISTRY
FRONTIERS

RESEARCH ARTICLE

View Article Online
View Journal | View Issue

Check for updates

Cite this: *Mater. Chem. Front.*, 2018, **2**, 296

Aggregation-responsive ON–OFF–ON fluorescence-switching behaviour of twisted tetrakis(benzo[*b*]furyl)ethene made by hafnium-mediated McMurry coupling†

Hiroyoshi Hamada,[a] Hayato Tsuji *[b] and Eiichi Nakamura *[a]

Received 3rd October 2017,
Accepted 17th November 2017

DOI: 10.1039/c7qm00453b

rsc.li/frontiers-materials

Fluorescence-switching dyes serve as important tools for bioimaging and environment sensing. Herein, we report a new type of molecule, tetrakis(benzo[*b*]furyl)ethene (**TBFE**), that undergoes two-wavelength ON–OFF–ON three-stage fluorescence switching triggered by aggregation. This compound features a sterically hindered tetrasubstituted ethene, made available by a hafnium-mediated McMurry coupling reaction. A fluorescent band of **TBFE** at 360 nm in THF disappears upon dilution with water towards 40% water in THF, giving way to a new peak at 510 nm. This switching behaviour is attributed to the combination of THF/H_2O ratio-dependent aggregation-caused quenching and aggregation-induced emission, as supported by the change of size distribution measured by dynamic light scattering and scanning electron microscopy.

Published on 27 novembre 2017. Downloaded on 2025-01-10 23:50:21.

Introduction

Environment-responsive fluorescent materials have attracted attention due to their chemical properties by themselves and for applications to bioimaging[1,2] and environmental sensing.[3,4] Aggregation-responsive dyes have been most widely studied for their fluorescence-switching property, and previous studies have focused on two-stage on–off switching, caused by either aggregation-caused quenching (ACQ) or aggregation-induced emission (AIE).[5] The former mechanism is generally found in planar π molecules,[6] while the latter in molecules with rotatable or vibratory units, such as tetraarylethenes (TAEs).[4,5] Three-stage switching[7] involving a continuous change of fluorescence has also been achieved by a combination of intramolecular charge transfer (ICT) and AIE.

Herein, we report a two-wavelength ON–OFF–ON fluorescence-switching behaviour of a new type of molecule, tetrakis(benzo[*b*]furyl)ethene (**TBFE**), triggered by aggregation (Fig. 1a). This compound features a sterically hindered tetrasubstituted ethene (Fig. 1b), made available by a hafnium-mediated McMurry coupling reaction. A fluorescence band of **TBFE** at 360 nm in THF disappears upon dilution with water towards 40% water in THF, giving way to a new peak at 510 nm (Fig. 1c). The intensity of the 360 nm fluorescence at 0% water weakens by 3.4 times at 40% water in THF, where the 510 nm fluorescence appears and its intensity increases by 9.8 times at 90% water. This switching behaviour is attributed to the combination of the ACQ effect of the 360 nm fluorescence and the AIE effect of the 510 nm fluorescence, as supported by the change of size distribution measured by dynamic light scattering (DLS) and scanning electron microscopy (SEM). This compound features a TAE as an AIE-phore framework (Fig. 1a, blue) and a benzofuran (BF) as a fluorescent unit (red), a class of fused furan compounds with high fluorescence quantum yield in solution and even in the solid state in some π-expanded molecules.[8] A key synthetic enabler of this research is the use of hafnium (Hf) for the

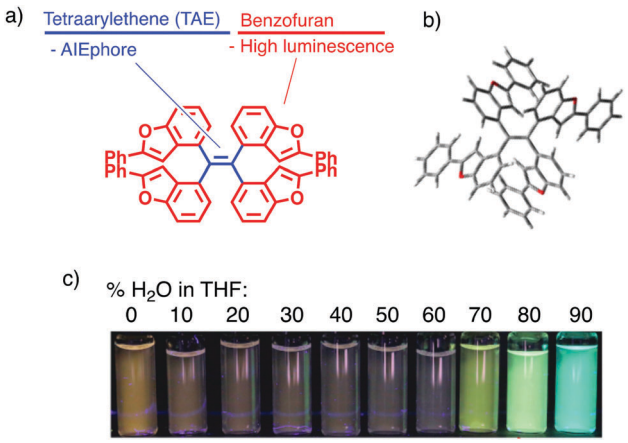

Fig. 1 Tetrakis(benzo[*b*]furyl)ethene (**TBFE**). (a) Molecular design. (b) Crystal structure showing twisting around the TAE centre (see ESI†). (c) Fluorescence intensity dependent on THF/H_2O ratio (excitation at 365 nm).

[a] *Department of Chemistry, The University of Tokyo, 7-3-1 Hongo, Bunkyo-ku, Tokyo 113-0033, Japan*
[b] *Department of Chemistry, Faculty of Science, Kanagawa University, 2946 Tsuchiya, Hiratsuka 259-1293, Japan. E-mail: tsujiha@kanagawa-u.ac.jp*

† Electronic supplementary information (ESI) available: Synthetic details, and geometry and measurement data. See DOI: 10.1039/c7qm00453b

This journal is © The Royal Society of Chemistry and the Chinese Chemical Society 2018

Published on 27 novembre 2017. Downloaded on 2025-01-10 23:50:21.

McMurry coupling, which we found useful for the synthesis of the sterically congested TAE core.

Results and discussion

Synthesis of TBFE

A retrosynthesis of **TBFE** calls for the deoxygenative McMurry-type coupling of two aryl ketone molecules (**7** in Scheme 1). To this end, we first prepared benzofuran **5** from a commercially available 3-bromophenol (**1**) in four steps *via* a procedure reported by Sanz *et al.*[9] Lithiation of **5** and nucleophilic addition of the resulting aryllithium to methyl formate gave alcohol **6**. Oxidation by MnO_2 afforded ketone **7**. The subsequent McMurry-type reductive coupling reaction of **7** was effectively promoted using $ZrCl_4$ or $HfCl_4$ with metallic Zn to obtain **TBFE** in 42% and 50% yields, respectively, whereas no reaction occurred with the use of the corresponding Ti reagent (Table 1). The use of zinc as a reducing reagent was inspired by Mukaiyama's protocol, where a combination of $TiCl_4$ and Zn was used.[10]

The high efficacy of the hafnium-mediated McMurry coupling was rather unexpected because of publications reporting the contrary.[11,12] We attribute the difference in efficacy among Ti, Zr, and Hf to the difference of atomic radius and/or the reducing ability of low-valent metal states. Zr and Hf with a larger atomic radius than Ti may be able to circumvent a steric problem encountered in the conventional Ti-mediated coupling known for its sluggishness upon the application to bulky ketones.[10,11] An alternative possibility includes the larger standard electrode potentials (M^{4+}/M) of Hf and Zn than Ti,[13] which provides a larger driving force for this deoxygenative reaction.

Optimized structure and UV absorption

Geometry optimization of **TBFE** at the B3LYP level of theory using the 6-31G* basis set showed that there are four stable conformational isomers within 4.28 kJ mol^{-1} (Fig. 1b and ESI,† Fig. S1–S5). In the most stable and hence most populated conformer, the 2-phenylbenzo[*b*]furan (BF) unit and the alkenyl C=C double bond of the alkene are twisted by 87.8° to each other. This optimized structure indicates that the π-conjugations of the BF unit have little electronic interaction with each other in the ground state, which accounts for the similarity of the absorption spectrum of **TBFE** in THF (Fig. 2a) to that of BF.

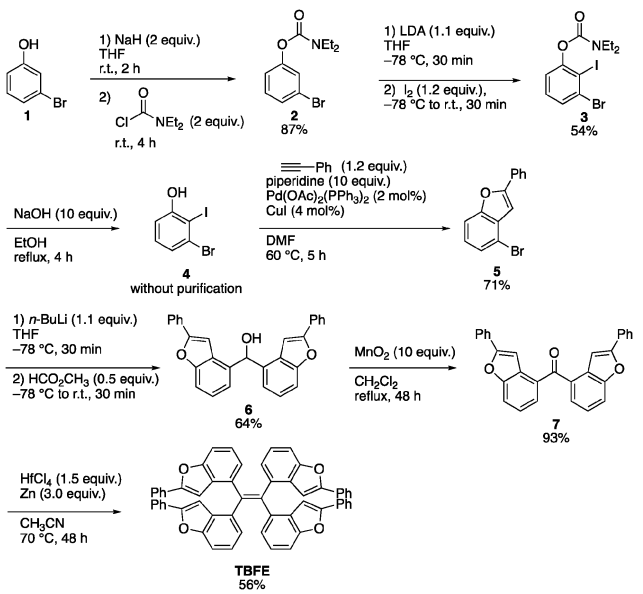

Scheme 1 Synthesis of **TBFE**.

Table 1 Group 4 metal-mediated McMurry-type coupling reactions of compound **7**

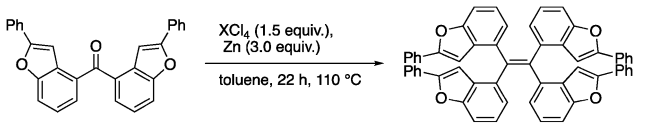

7 **TBFE**

XCl_4	r^a (pm)	$E_{M^{4+}/M}{}^b$ (V)	Yield (%)
$TiCl_4$	148	−1.37	0
$ZrCl_4$	164	−1.45	42
$HfCl_4$	164	−1.55	50

[a] Atomic radius of metal. [b] Standard electrode potential of group 4 metals.[13]

Fluorescence switching in THF/H_2O

TBFE shows two-wavelength ON–OFF–ON switching behaviour of its fluorescence in a THF/H_2O mixed-solvent system (Fig. 1c and 2b, c), while the maximum absorption wavelength around 317 nm remains unchanged for THF/H_2O volume ratios from 0% to 90% (Fig. 2a). In pure THF (Fig. 2b, blue line and Fig. 2c, blue dot), we see a fluorescence peak at 360 nm due to emission from the BF moieties (ESI,† Fig. S7) with a fluorescence quantum yield (Φ_{FL}) of 0.094. Upon gradual dilution with H_2O, the intensity of the emission band decreases to Φ_{FL} = 0.028 at 40% water. At 70% water (purple dot in Fig. 2c), however, a new peak appears around 530 nm with Φ_{FL} of 0.159, which undergoes a gradual blueshift and intensifies as the H_2O ratio is increased. At a 90% H_2O ratio, a well-defined signal at 503 nm appears with Φ_{FL} = 0.263, accompanied by a slight blueshift to 503 nm. At this ratio, the peak at 360 nm was not seen at all; **TBFE** precipitates in pure water.

We surmise that this ON–OFF–ON switching behaviour originates from the aggregation of **TBFE**, which causes ACQ of the 360 nm fluorescence, and AIE of the 510 nm emission. There was no redshift of the 360 nm fluorescence band at 0% to 40% water, suggesting that an ICT process, which generally causes a redshift,[7] is not responsible for the observed switching phenomenon. The lack of CT participation in the present switching phenomenon was suggested by a solvatochromic study. Thus, the fluorescence spectra of **TBFE** in polar and nonpolar solvents for a range of relative permittivities from 2.02 to 26 showed only a 10 nm variation of the fluorescence maxima (ESI,† Fig. S9), indicating also that the photoexcited states of **TBFE** are rather nonpolar.[14]

Fluorescence lifetime measurements in THF and THF/H_2O mixed solvents (50, 70, 90% water) afforded further insights on the photophysical properties of **TBFE**. First, significantly slower nonradiative decay in the THF/H_2O mixed solvents than in THF

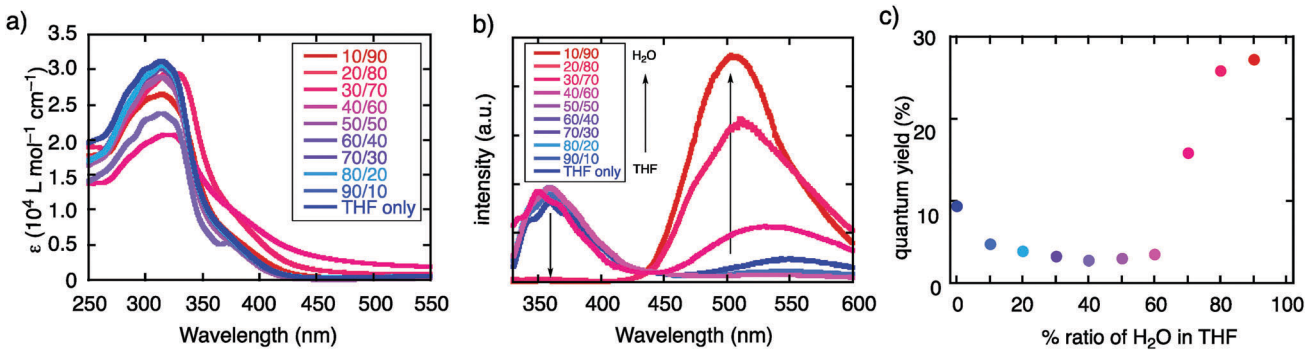

Fig. 2 Photophysical properties of **TBFE** in a THF/H_2O mixed solvent system. (a) Absorption spectra (1.0×10^{-5} M), (b) fluorescence spectra (1.0×10^{-6} M, λ_{ex} = 317 nm), and (c) transition of photoluminescence quantum yield measured by the absolute method.

Published on 27 novembre 2017. Downloaded on 2025-01-10 23:50:21.

Table 2 Fluorescence quantum yield Φ_{FL}, average fluorescence lifetime $\langle\tau\rangle$, radiative rate constant k_r, and nonradiative rate constant k_{nr} of **TBFE** and BF

	TBFE				BF
	In THF	In THF/H_2O (50/50)	(30/70)	(10/90)	In THF
Φ_{FL}	0.094	0.050	0.159	0.273	0.656
$\langle\tau\rangle$ (ns)	1.2	1.3	1.6	2.9	1.2
k_r (10^7 s^{-1})[a]	7.8	3.8	9.7	9.5	55
k_{nr} (10^7 s^{-1})[a]	75	72	51	25	29

[a] Calculated from Φ_{FL} and τ.

was observed, which is a signature of AIE processes.[4,5,15] The nonradiative rate constant (k_{nr}) did not decrease by water addition in 0–50% water ratio. At 70% water, where the AIE effect was seen in the fluorescence spectra, a decrease in k_{nr} was observed as well. Further water addition dropped the k_{nr} at 90% water to about one-third of that in THF (ESI,† Table S10), calculated from their Φ_{FL} and average lifetimes ($\langle\tau\rangle$), while the radiative rate constant (k_r) did not change significantly. Second, the rather low fluorescence quantum yield of **TBFE** in THF compared with the parent BF in the same solvent is attributable to both larger k_{nr} and smaller k_r of **TBFE** than those of BF. Interestingly, the k_{nr} value at 90% water where **TBFE** is aggregated was the same as that of BF in THF. The large k_{nr} value at 70% indicates that molecules are still not as densely aggregated as at 90% water. Time-dependent density functional theory calculations for each conformer of **TBFE** showed much smaller oscillator strengths for S_0–S_1 excitation than for BF (ESI,† Table S7). Third, the decay curves at 70–90% water were fitted with a biexponential function while the curves in pure THF and at 50% water were fitted with a monoexponential function. This difference in the fitting indicates that **TBFE** forms two major conformers in the aggregated state through suppression of intramolecular bond rotation to afford conformers that are energetically close to each other (Table 2).

Dynamic light scattering and scanning electron microscopy observation

The above spectral evidence of aggregation-induced changes was supported by direct observation of the aggregation behaviour by DLS and SEM. Thus, the observed size distribution of aggregates of **TBFE** in THF/H_2O matched the switching behaviour of the fluorescence spectra, supporting the aggregation-induced mechanism that we are proposing here. In the low H_2O ratio (0–50%), molecules are either dissolved unimolecularly or form aggregates made of several molecules, as indicated by the DLS size distribution observed in the region below 10 nm (Fig. 3a, bottom). When the H_2O ratio reached 60%, the size distribution suddenly became larger than 10^3 nm. In the high H_2O ratio region (>60%), the size decreased gradually from a maximum[16] of 4.8×10^3 nm at 60% to 8.3×10^2 nm at 90% (Fig. 3a, top). This is probably because the hydrophobic **TBFE** aggregates more

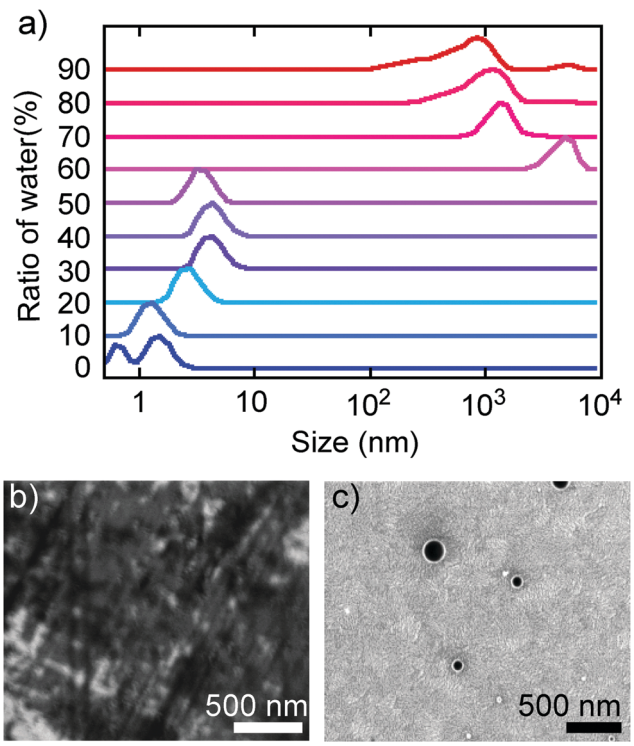

Fig. 3 Aggregation behaviour of **TBFE**. (a) Size distribution in THF/H_2O solvents obtained by DLS measurements. This figure was obtained as a correlation function (Fig. S11, ESI†) and outputted as a volume distribution. (b and c) SEM images of **TBFE** on ITO formed by spin-coating using THF and THF/H_2O = 10/90, respectively. The scale bars are 500 nm.

 This journal is © The Royal Society of Chemistry and the Chinese Chemical Society 2018

Published on 27 novembre 2017. Downloaded on 2025-01-10 23:50:21.

compactly in the aqueous solution due to surface tension.[17] Hence, the side units of **TBFE** would not be sufficiently fixed, and its fluorescence spectrum was similar to that of the disaggregated state (in Fig. 2b and 3a, H_2O ratio = 60%). SEM of the THF/H_2O solution of **TBFE** spin coated on ITO supported the DLS observations. The sample in pure THF showed only amorphous domains on ITO (Fig. 3b), the sample in THF/H_2O (10/90) showed spherical aggregates of 50–300 nm (Fig. 3c and ESI,† Fig. S12). This diameter matches the data from DLS. No sharp diffraction peak in the powder X-ray diffraction pattern of the **TBFE** aggregates in THF/H_2O (10/90) indicates that the molecules are amorphous in the aggregates (ESI,† Fig. S14).

Conclusion

In summary, we found an intriguing example of two-wavelength ON–OFF–ON three-stage fluorescence switching triggered by the aggregation for a new TAE derivative, **TBFE**, in a THF/H_2O mixed-solvent system. The THF/H_2O ratio-dependent change of size distribution found by DLS and SEM suggests that the fluorescence switching is caused by the combination of ACQ and AIE. The similarity of the photophysical properties of **TBFE** in THF to those of 2-phenylbenzo[*b*]furan and the absence of solvatochromic shift also support that ICT, which has been widely found in such switching phenomena, does not participate in the present system. The Hf-mediated McMurry-type coupling developed for the **TBFE** synthesis exploits the large atomic radius and high reduction capability of the Hf metal and will expand the synthetic scope of this classical method towards the synthesis of tetrasubstituted ethenes with bulky substituents.

Conflicts of interest

There are no conflicts to declare.

Acknowledgements

This work was supported by Grants-in-Aid for Scientific Research (no. 15H05754 for EN, and no. 15H00987 and 17H05163 to HT on Innovative Areas ''π-System Figuration: Control of Electron and Structural Dynamism for Innovative Functions'').

Notes and references

1 (*a*) N. Fernándes-Suárez and A. Y. Ting, *Nat. Rev. Mol. Cell Biol.*, 2008, **9**, 929–943; (*b*) G. D. Liang, J. W. Y. Lam, W. Qin, J. Li, N. Xie and B. Z. Tang, *Chem. Commun.*, 2014, **50**, 1725–1727.
2 M. Irie, T. Fukaminato, K. Matsuda and S. Kobatake, *Chem. Rev.*, 2014, **114**, 12174–12277.
3 (*a*) S. Sasaki, G. P. C. Drummen and G.-i. Konishi, *J. Mater. Chem. C*, 2016, **4**, 2731–2743; (*b*) S. Chen, Y. Hong, Y. Liu, J. Liu, C. W. T. Leung, M. Li, R. T. K. Kwok, E. Zhao, J. W. Y. Lam, Y. Yu and B. Z. Tang, *J. Am. Chem. Soc.*, 2013, **135**, 4926–4929; (*c*) Y. Hong, S. Chen, C. W. T. Leung, J. W. Y. Jam, J. Liu, N.-W. Tseng, R. T. K. Kwok, Y. Yu, Z. Wang and B. Z. Tang, *ACS Appl. Mater. Interfaces*, 2011, **3**, 3411–3418.
4 J. Mei, Y. Hong, J. W. Y. Lam, A. Qin, Y. Tang and B. Z. Tang, *Adv. Mater.*, 2014, **26**, 5429–5479.
5 J. Mei, N. L. C. Leung, R. T. K. Kwok, J. W. Y. Lam and B. Z. Tang, *Chem. Rev.*, 2015, **115**, 11718–11940.
6 H. Tong, Y. Dong, Y. Hong, M. Häussler, J. W. Y. Lam, H. H.-Y. Sung, X. Yu, J. Sun, I. D. Williams, H. S. Kwok and B. Z. Tang, *J. Phys. Chem. C*, 2007, **111**, 2287–2294.
7 (*a*) S. J. Ananhakrishnan, E. Varathan, E. Ravindran, N. Somanathan, V. Subramanian, A. B. Mandal, J. D. Sudha and R. Ramakrishnan, *Chem. Commun.*, 2013, **49**, 10742–10744; (*b*) Y. Li, Y. Wu, J. Chang, J. Chen, L. Liu and F. Li, *Chem. Commun.*, 2013, **49**, 11335–11337; (*c*) E. Wang, J. W. Y. Lam, R. Hu, C. Zhang, Y. S. Zhao and B. Z. Tang, *J. Mater. Chem. C*, 2014, **2**, 1801–1807; (*d*) R. Hu, E. Lager, A. Aguilar-Aguilar, J. Liu, J. W. Y. Lam, H. H. Y. Sung, I. D. Williams, Y. Zhong, K. S. Wong, E. Peña-Cabrera and B. Z. Tang, *J. Phys. Chem. C*, 2009, **113**, 15845–15853.
8 (*a*) N. Hayashi, Y. Saito, H. Higuchi and K. Suzuki, *J. Phys. Chem. A*, 2009, **113**, 5342–5347; (*b*) N. Hayashi, Y. Saito and H. Higuchi, *Heterocycles*, 2009, **77**, 1261–1268; (*c*) H. Tsuji and E. Nakamura, *Acc. Chem. Res.*, 2017, **50**, 396–406.
9 R. Sanz, M. P. Castroviejo, Y. Fernández and F. J. Fañanás, *J. Org. Chem.*, 2005, **70**, 6548–6551.
10 T. Mukaiyama, T. Sato and J. Hanna, *Chem. Lett.*, 1973, 1041–1044.
11 (*a*) J. E. McMurry, *Chem. Rev.*, 1989, **89**, 1513–1524; (*b*) M. Ephritikhine, *Chem. Commun.*, 1998, 2549–2554.
12 R. Dams, M. Malinowski and H. J. Geise, *Bull. Soc. Chim. Belg.*, 1982, **91**, 19–152.
13 *CRC Handbook of Chemistry and Physics*, ed. W. M. Haynes, CRC Press, Boca Ration FL, 92nd edn, 2011, pp. 8-20–8-29.
14 S. Nigam and S. Rutan, *Appl. Spectrosc.*, 2001, **55**, 362–370.
15 Y. Ren, J. W. Y. Lam, Y. Dong, B. Z. Tang and K. S. Wong, *J. Phys. Chem. B*, 2005, **109**, 1135–1140.
16 K. Harano, T. Homma, Y. Niimi, M. Koshino, K. Suenaga, L. Leibler and E. Nakamura, *Nat. Mater.*, 2012, **11**, 877–881.
17 T. V. Chalikian, *J. Phys. Chem. B*, 2001, **105**, 12566–12578.